

Planar Spiral Coil Design for a Pulsed Induction Metal Detector to Improve the Sensitivities

Bobae Kim, *Student Member, IEEE*, Seung-hoon Han, and Kangwook Kim, *Member, IEEE*

Abstract—In a pulsed induction metal detector system, the sensitivity variation for detectable minimum metal target and the maximum detection distance are investigated as the winding geometry of the search coil is varied. A number of planar square spiral mono coils with various fill ratios and wire spacing-to-width ratios are comparatively analyzed based on a numerical simulation. Five representative coils are fabricated and applied to a pulsed induction metal detector system as a search coil. It is demonstrated that a search coil with a larger fill ratio has a high size sensitivity for a minimum metal target at close distances, which may be missed by coils with smaller fill ratios. A search coil with a smaller wire spacing-to-width ratio is shown to have a high depth sensitivity for maximum detection distances.

Index Terms—Detector sensitivity, electromagnetic induction coil, landmine detection, pulsed induction metal detector.

I. INTRODUCTION

HUMANITARIAN demining is a significant international issue. For the effective detection of buried landmines, various sensor technologies have been employed [1], [2]. The most widely used sensor for mine detection is the metal detector, which uses the principle of electromagnetic induction (EMI). In a metal detector, the time-varying magnetic field generated by the transmitter (Tx) coil induces an eddy current in the metal components of a landmine. The secondary magnetic field generated by the eddy current is detected by the receiver (Rx) coil. The two coils are usually located very close to each other, and they are often collectively called a search coil.

The performance of a metal detector can be measured in terms of its depth and size sensitivities. The depth sensitivities of detectors can be compared in terms of the maximum detection distance between the search coil and a metal target. Metal detectors with a higher depth sensitivity can detect a target at a deeper depth compared to those with a lower depth sensitivity. The size sensitivities can be compared in terms of the minimum size of

the target at a distance close to the search coil. Metal detectors with a higher size sensitivity can detect a smaller target than those with a lower size sensitivity [3], [4].

The sensitivities of a metal detector depend heavily on the distribution of the magnetic field that is generated by the search coil. Thus, the search coil characteristics, such as the configuration and size, are directly related to the detector sensitivities, although they are influenced by numerous external (e.g., the target properties and soil conditions) and internal conditions (e.g., the search coil characteristics, transmitter current, signal-to-noise ratio, and signal processing method). The detector sensitivities according to the coil configuration and size can be found in literature [5]–[7].

The detector sensitivities are also influenced by the winding geometry of the search coil as well as the coil configuration and size because the distribution of the magnetic field depends on the current distribution, which is determined by the coil winding pattern [8], [9]. Thus, the purpose of this study is to investigate the variations of the detector sensitivities as the winding geometry of the search coil is varied. The winding geometry is parameterized by two ratios: the fill ratio and the spacing-to-width ratio.

II. SEARCH COIL GEOMETRIES AND FIELD STRENGTHS

In this letter, planar square spiral mono coils with an outer side length of 45 cm are considered as the search coil. The geometry of the planar square spiral coil can be described by the outer side length (D_{out}), the inner side length (D_{in}), the number of turns (N), the wire width (w), and the wire spacing (s), as shown in Fig. 1. The fill ratio is defined as

$$\rho = \frac{D_{out} - D_{in}}{D_{out} + D_{in}}. \quad (1)$$

In this section, the magnetic field strength is investigated as the fill ratio and the spacing-to-width ratio are varied. The magnetic fields are obtained by modeling the coils in the ANSYS Maxwell magnetostatic solver.

A. Effect of the Fill Ratio

To investigate the effect of the fill ratio on the magnetic field distribution induced by the search coil, the fill ratio is varied from 0.27 to 0.83, while the coil inductance and the spacing-to-width ratio are fixed at approximately 150 μH and $s/w = 1$, respectively. The inner side length, wire width, wire spacing, and number of turns are determined accordingly. Table I shows the geometrical parameters of three representative cases. Table I also shows the calculated and measured

Manuscript received April 29, 2014; accepted July 15, 2014. Date of publication July 22, 2014; date of current version August 08, 2014. This work was supported in part by the Agency for Defense Development under Contract No. UC120055ID and Samsung Thales Corporation, Korea, under Contract No. STC-C-13-003.

B. Kim and K. Kim are with the School of Mechatronics, Gwangju Institute of Science and Technology (GIST), Gwangju 500-712, Korea (e-mail: mkkim@gist.ac.kr).

S.-H. Han is with the ISR-PGM R&D Center, Samsung Thales Corporation, Yongin City 449-880, Korea (e-mail: sh0518.han@samsung.com).

Color versions of one or more of the figures in this letter are available online at <http://ieeexplore.ieee.org>.

Digital Object Identifier 10.1109/LAWP.2014.2341591

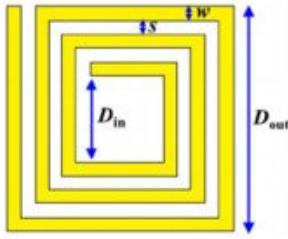


Fig. 1. Geometrical parameters of the planar square spiral coil.

TABLE I
SEARCH COIL PARAMETERS WITH VARIOUS FILL RATIOS

	unit	Coil 1	Coil 2	Coil 3			
D_{in}	cm	25.8	15.4	4.2			
w	mm	3.1	3.8	4			
s	mm	3.1	3.8	4			
N	-	16	20	26			
ρ	-	0.27	0.49	0.83			
s/w	-	1	1	1			
		Calc.	Meas.	Calc.	Meas.	Calc.	Meas.
L	μH	152	150	151	149	149	152
R	Ω	0.9	1.8	0.9	1.7	1	1.7

equivalent circuit parameters for the coils when they are modeled as the series inductance (L) and resistance (R), which can be calculated as follows:

$$L = K_1 \mu_0 \frac{N^2 (D_{out} + D_{in})}{2(1 + K_2 \rho)} \quad (2)$$

and

$$R = \rho_c \frac{l_c}{w \cdot t_c} \quad (3)$$

where the coefficients K_1 and K_2 are 2.34 and 2.75 for square coils, respectively; ρ_c is the resistivity of the wire; and l_c is the total wire length [10], [11].

Fig. 2 shows the magnetic field strengths of the coils 1, 2, and 3 as a function of the distance along the coil axis (z -axis). The current in the coil is normalized to 1 A for all coils. The figure shows that the magnetic field strength decays as the distance increases. At a distance greater than 300 mm, the magnetic field strengths of the three coils seem to be essentially the same. However, at close distances, the magnetic field strengths are stronger with a higher fill ratio.

This is related to the sizes of the loops consisting of the multi-turn coils, which can be considered as a superposition of single-loop coils with different sizes. Typically, the magnetic field of a smaller coil is relatively strong at a close distance as compared to that of a larger coil. However, the magnetic field of a smaller coil decays more rapidly as the distance increases than that of a larger coil. Thus, at far distances, the field generated by the large outer loops is dominant. Because the sizes of the outer loops are all the same in Fig. 2, the magnetic field strengths are essentially the same at far distances.

At close distances, however, the smaller inner loops generate stronger fields than the outer loops. Thus, the coils with a higher fill ratio generate stronger fields than those with a lower fill ratio.

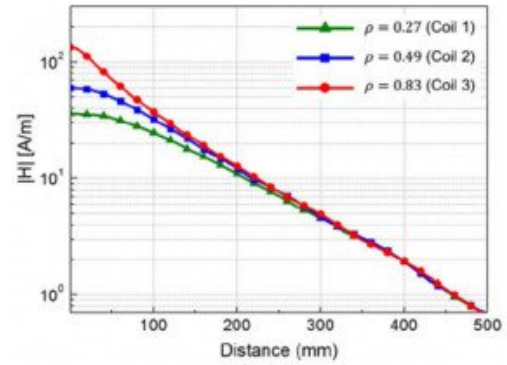
Fig. 2. Plots of the magnetic field strength along the z -axis for search coils with various fill ratios (ρ).

TABLE II
SEARCH COIL PARAMETERS WITH VARIOUS SPACING-TO-WIDTH RATIOS

	unit	Coil 4	Coil 3	Coil 5			
D_{in}	cm	4.2	4.2	4.6			
w	mm	4	4	4			
s	mm	6	4	2			
N	-	21	26	34			
ρ	-	0.83	0.83	0.82			
s/w	-	1.5	1	0.5			
		Calc.	Meas.	Calc.	Meas.	Calc.	Meas.
L	μH	97	98	149	152	261	264
R	Ω	0.7	1.4	1	1.7	1.5	2.3

Because the eddy current in the target is strongly related to the magnetic field strength, the coils with a higher fill ratio are considered to have a higher size sensitivity at a close distance than those with a lower fill ratio.

B. Effect of the Spacing-to-Width Ratio

To investigate the effect of the spacing-to-width ratio (s/w) on the magnetic field distribution, the wire spacing-to-width ratio is varied from 0.5 to 1.5. Other parameters are determined such that the fill ratio and wire width are approximately 0.83 and 4 mm, respectively. Table II shows the geometrical parameters and equivalent circuit parameters for three representative coils.

Fig. 3 shows the magnetic field strengths of coils 3, 4, and 5 as a function of the distance along the coil axis. The figure shows that a coil with a smaller spacing-to-width ratio has a stronger magnetic field for the entire observed distance range.

With other parameters fixed, decreasing the spacing-to-width ratio results in an increase of the number of turns. Because each turn of the loop carries essentially the same amount of current, the magnetic field is increased. Thus, a coil with a smaller wire spacing-to-width ratio can have a higher depth sensitivity.

However, when a search coil with a large number of turns is applied to a PI metal detector system, it is difficult to rapidly turn off the transmitter current in the coil due to the long time constant of the coil. In this case, the target eddy current detected by the receiver coil may be overwhelmed by the residual current in the transmitter coil. Therefore, the actual performance of the coils needs to be experimentally verified in an actual system.

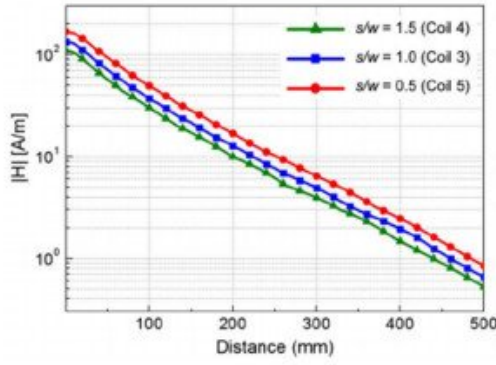


Fig. 3. Plots of the magnetic field strength along the z -axis for search coils with various spacing-to-width ratios, s/w .

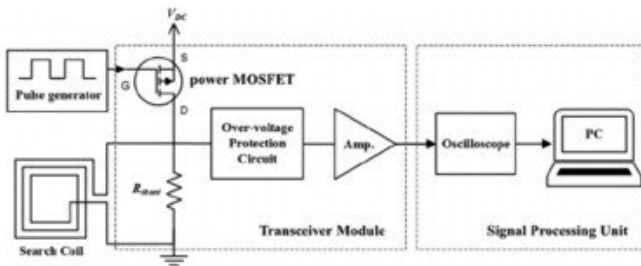


Fig. 4. Simplified block diagram of a PI metal detector system.

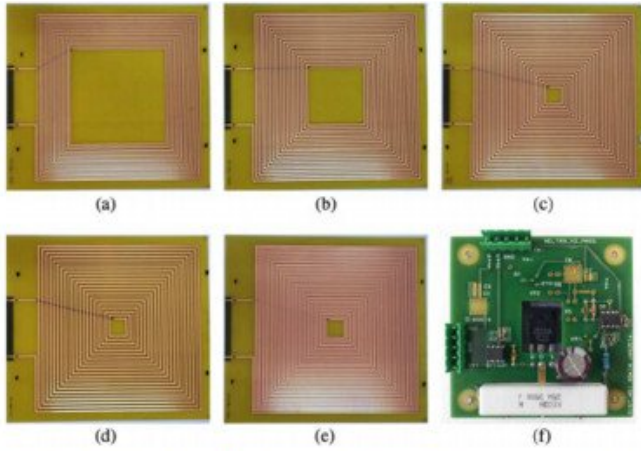


Fig. 5. Fabricated (a) coil 1 ($\rho = 0.27$), (b) coil 2 ($\rho = 0.49$), (c) coil 3 ($\rho = 0.83$), (d) coil 4 ($s/w = 1.5$), (e) coil 5 ($s/w = 0.5$), and (f) the transceiver module.

III. EXPERIMENTAL RESULTS ON DETECTOR SENSITIVITIES

In an effort to investigate the effect of the coil winding geometry on actual detector sensitivities, the coils described in Tables I and II were fabricated on an FR-4 printed circuit board with a copper thickness of 2 oz. The coils were then applied to a PI metal detector system. Fig. 4 shows a simplified block diagram of the PI metal detector system, which consists of a search coil, a transceiver module, and a signal processing unit. The photographs of the five coils are shown in Fig. 5(a)–(e), and the transceiver module is shown in Fig. 5(f).

In the transceiver module, a power metal oxide semiconductor field-effect transistor (MOSFET; IXTX32P60P, IXYS

TABLE III
MEASURED DETECTION RESULTS OF VARIOUS INSCOILS

Inscoil		-	Coil 1	Coil 2	Coil 3	Coil 4	Coil 5
Name	Diameter (cm)	ρ	0.27	0.49	0.83	0.83	0.82
		s/w	1	1	1	1.5	0.5
O_I	1.40	-	X	O	O	O	O
M_I	1.24	-	X	O	O	O	O
K_I	0.95	-	X	X	O	O	O
I_I	0.70	-	X	X	X	X	X

Corporation) was used to switch on/off the current flow in the search coil. The switch state is determined by the voltage from the pulse generator, which consists of a MOSFET driver and a waveform generator. The pulse generator provides a continuous pulse train with a repetition frequency of 1 kHz and a pulse width of 700 μ s.

For each coil, the supply voltage, V_{DC} , is adjusted such that a peak current of 5 A flows in the coil. A shunt resistor (R_{shunt}) was placed across the search coil to reduce voltage ringing upon switching off due to the parasitic capacitance of the coil. The values of the shunt resistors are 240 Ω for coils 1–4, and 350 Ω for coil 5. The voltage on the search coil is fed into the amplifier through an over-voltage protection circuit.

The output signal of the amplifier was acquired by an Agilent DSO7106A oscilloscope. The LabVIEW software on a PC was used for the signal processing for target detection. The decision for target detection was made based on the root mean square (RMS) taken from the exponentially weighted output voltage from $t_1 = 10 \mu$ s to $t_2 = 310 \mu$ s after the switch was turned off; i.e.,

$$v_{rms} = \sqrt{\frac{1}{T} \int_{t_1}^{t_2} s^2(t) e^{-(t_2-t)/T} dt} \tag{4}$$

where $s(t)$ is the output voltage and $T = t_2 - t_1$ is the averaging period [12]. If the real-time RMS value is larger than the RMS taken without a target, a positive decision is made.

To measure the size sensitivity for the minimum metal target at a close distance, four types of Inscoil (O_I , M_I , K_I , and I_I), which are short-circuited loops of wire reported in [13], were used instead of minimum metal mines. Table III shows the measured detection results of each coil for the various Inscois. The labels “O” and “X” denote a detection and a miss, respectively. The distance of the target is 2.5 cm from the coil.

In Table III, coils 1–3 are a group of search coils with varying fill ratios. It can be seen that the coils with higher fill ratios can detect smaller targets than those with lower fill ratios. For example, the coil with the fill ratio of 0.83 (coil 3) can detect Inscois O_I , M_I , and K_I . In contrast, the coil with the fill ratio of 0.27 (coil 1) cannot detect any Inscois. Thus, it is demonstrated that a coil with a higher fill ratio has higher size sensitivity for a minimum metal target at a close distance.

Coils 3–5 are another group of search coils for which the wire spacing-to-width ratio varies. These coils showed the same results with regard to Inscoil detection. Thus, the spacing-to-width ratio has little effect on the size sensitivity for a minimum metal target.

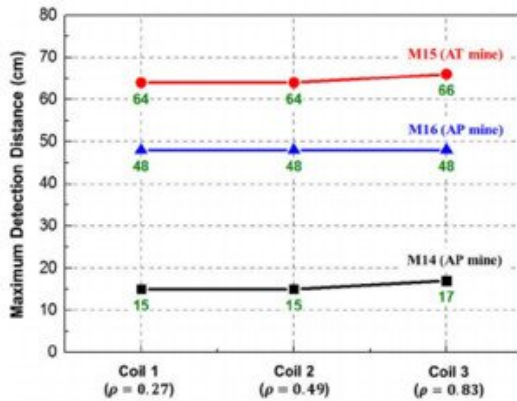


Fig. 6. Measured maximum detection distance of the coils for M14, M15, and M16 landmines according to various fill ratios, ρ .

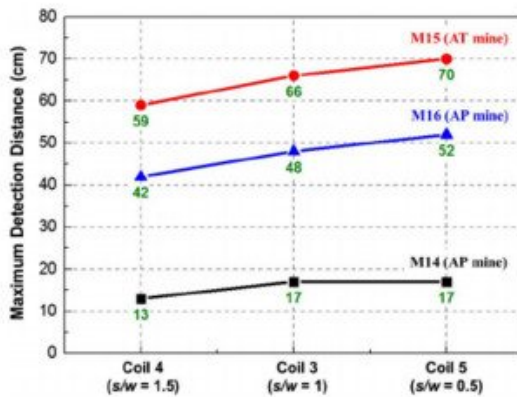


Fig. 7. Measured maximum detection distance of the coils for M14, M15, and M16 landmines according to the wire-spacing-to-width ratio, s/w .

To investigate the depth sensitivity, the maximum detection distance of the PI metal detector was measured in air for various targets: an M14 anti-personal (AP) mine, an M16 AP mine, and an M15 anti-tank (AT) mine. Fig. 6 shows the variation of the maximum detection distance of coils 1–3, which have different fill ratios. For all coils, the M15, which is the largest among the targets, has the longest maximum detection distance, while M14, which is the smallest target, has the shortest maximum detection distance. On the other hand, the maximum detection depth is hardly influenced by the fill ratio because, as discussed in Section II, the magnetic field strengths of the three coils are essentially the same as the distance is increased.

Fig. 7 demonstrates the variation of the maximum detection distance for the wire spacing-to-width ratios (s/w 's) of coils 3–5. Coil 4, with a wire spacing-to-width ratio of 1.5, had detection depths of 13, 42, and 59 cm for the M14, M16, and M15 mines, respectively. On the other hand, the detection distance of the coil 5, which has $s/w = 0.5$, is increased to 17 cm for the M14 mine, 52 cm for the M16 mine, and 70 cm

for the M15 mine. This confirms that coils with a smaller wire spacing-to-width ratio have a higher depth sensitivity. These results were in agreement with the predictions made by the static magnetic field simulation, as explained in Section II.

IV. CONCLUSION

In this letter, we investigated the variations of the detector sensitivities as the winding geometry of the search coil is varied. The winding geometry is determined by two ratios, i.e., the fill ratio and the wire spacing-to-width ratio, and the size and depth sensitivities of coils with different ratios are investigated through numerical simulations and experiments.

Consequently, with regard to the size sensitivity for the minimum metal target at a close distance, a coil with a higher fill ratio is shown to have higher size sensitivity. It was also shown that the size sensitivity is hardly influenced by the spacing-to-width ratio. On the other hand, with regard to the depth sensitivity for the maximum detection distance, a coil with a smaller wire spacing-to-width ratio is shown to have a higher depth sensitivity, and the depth sensitivity was hardly affected by the fill ratio.

REFERENCES

- [1] J. MacDonald and J. R. Lockwood, *Alternatives for Landmine Detection*. Santa Monica, CA, USA: RAND Corp., 2003.
- [2] C. Gooneratne, S. Mukhopahyay, and G. Sen Gupta, "A review of sensing technologies for landmine detection: Unmanned vehicle based approach," in *Proc. 21st Int. Conf. Auton. Robots Agents*, Palmerston North, New Zealand, Dec. 2004, pp. 401–407.
- [3] D. Guelle, *Metal Detector Handbook for Humanitarian Demining*. Luxembourg, Norwich: Office for Official Publications of the European Communities, 2003.
- [4] "Humanitarian mine action—Test and evaluation—Part 1: Metal detectors," CEN Workshop Agreement, CWA 14747-1, 2003.
- [5] C. Bruschini, "A multidisciplinary analysis of frequency domain metal detectors for humanitarian demining," Ph.D. dissertation, Vrije Univ., Brussels, Belgium, 2002.
- [6] C. Moreland, "Coil basics," *Geotech, Tech. Rep.*, 2006 [Online]. Available: http://northeastmetaldetecting.com/downloads_pdf_files/coils.pdf
- [7] Deeptech Metal Detectors, "Metal detectors coil and search head design—Patents and utility models," Whitepaper, 2007.
- [8] C. Fernandez *et al.*, "Design issues of a core-less transformer of a contactless application," in *Proc. 17th Annu. IEEE APEC Expo*, Mar. 2002, vol. 1, pp. 339–345.
- [9] J. M. Lopez-Villegas, J. Samitier, C. Cane, and P. Losantos, "Improvement of the quality factor of RF integrated inductors by layout optimization," in *Proc. Int. Microw. Symp.*, Jun. 1998, pp. 169–172.
- [10] S. S. Mohan, M. M. Hershenson, S. P. Boyd, and T. H. Lee, "Simple accurate expression for planar spiral inductances," *IEEE J. Solid-State Circuits*, vol. 34, no. 10, pp. 1419–1424, Oct. 1999.
- [11] U.-M. Jow and M. Ghovanloo, "Design and optimization of printed spiral coils for efficient transcutaneous inductive power transmission," *IEEE Trans. Biomed. Circuits Syst.*, vol. 1, no. 3, pp. 193–202, Sep. 2007.
- [12] R. Yates, "Exponential RMS detector (ExpRMS)," 2007 [Online]. Available: <http://www.digitalsignallabs.com/alg.pdf>
- [13] Department of Defense's Unexploded Ordnance Center of Excellence (UXOCOE), "Scientific and technical report page for simulants mines," 1998 [Online]. Available: <http://www.gichd.org/fileadmin/GICHD-resources/rec-documents/SimulantMines.pdf>